Functional Groups on the Surface of Carbonaceous Nanomaterials and Human Health

Ari Setyan[1], Jean-Jacques Sauvain[2], Michael Riediker[2], Olga Popovicheva[3] and Michel J. Rossi[4]
1 Université du Littoral Côte d'Opale (ULCO), 59140 Dunkerque, France
2 Institut Universitaire Romand de Santé au Travail (IST), 1000 Lausanne, Switzerland
3 Moscow State University, Institute of Nuclear Physics, 119991 Moscow, Russia
4 Paul Scherrer Institute (PSI), 5232 Villigen PSI, Switzerland
michel.rossi@psi.ch

The combustion conditions of hydrocarbon flames determine to a large extent the bulk and interfacial properties of the resulting combustion aerosol (soot). We have applied a soft interrogation technique for some of the interfacial functional groups using heterogeneous reactions of six probe gases of differing reactivity, namely $N((CH_3)_3)$, NH_2OH, CF_3COOH, HCl, NO_2, O_3. The experimental method rests upon measuring the rate of uptake of a probe gas under molecular flow conditions in the presence of deposited aerosol particles whose metrology is known (mass, specific surface area). The gas uptake to saturation of the probe molecules was measured in a Knudsen flow reactor and expressed as a density of surface functional groups using the measured BET surface area. The experimental methodology also afforded the measurement of the uptake coefficient of the probe gas to the carbonaceous nanoparticle.

The probe gases taken up by the sample addressed acidic (carboxylic) and basic sites such as pyrones, carbonyl or partially oxidized sites (R_1-C(O)-R_2) and strongly/weakly reducing functional surface groups. The used probes enabled the characterization of the particle surface in terms of its oxidation state (oxidized, partially oxidized, strongly/weakly reducing). The limit of detection was generally well below 1% of a molecular monolayer depending on the BET surface area of the used soot. The soot samples interacted with all probe gases which points to the coexistence of many different functional groups on the same aerosol surface such as acidic, basic, strongly/weakly reducing and oxidizing sites.

Table 1 displays the experimental results on four soot reference materials as well as three multiwalled carbon nanotubes (MWCNT). The salient differences between these carbonaceous materials will be discussed in some detail. For instance, The 5% BTCA-doped Graphitized Thermal Soot (GTS80) showed in fact 17% of a molecular monolayer of carboxylic surface functions, roughly 50 times the amount of the undoped substrate material GTS80 and a factor of 5 more than polyacrylic acid-coated MWCNT. For O_3 and NO_2 exposure to reference soot a slow steady-state reaction has been measured corresponding to a first-order uptake coefficient of roughly $4x10^{-5}$. It is interesting to note that no significant uptake of HCl has been measured in contrast to CF_3COOH which may indicate the presence of basic oxides on the soot. These compounds are derived from α- or γ-pyrone of which coumarin and chromone are aromatic derivatives. This basicity is based on a special topology between a carbonyl and an ether function and does not necessitate the presence of an amine N.

Table 1 : Surface functional group densities for six different gas probes for soot and MWCNT's. The upper and lower numbers in each box correspond to the number of molecules/cm^2 and the fractional surface coverage in monolayers, respectively. The red numbers indicate steady-state uptake (reaction).

Samples → Probes ↓	Graphitized Thermal Soot GTS6 (6 m^2/g)	Thermal Soot T900 (6.5 m^2/g)	Graphitized Thermal Soot GTS80 (80 m^2/g)	GTS80 + 5% BTA (80 m^2/g)	MWCNT 1 Uncoated (227.4 m^2/g))	MWCNT 2 Polyacid Polmer Coating (54.1 m^2/g)	MWCNT 3 PS-PB-PMMA Coating (34 m^2/g)
$N(CH_3)_3$			$1.1x10^{12}$ 0.0030	$6.1x10^{13}$ 0.1690	$1.3x10^{12}$ 0.0036	$1.2x10^{13}$ 0.033	$8.0x10^{11}$ 0.0022
NH_2OH			$4.0x10^{12}$ 0.005	$2.9x10^{13}$ 0.037	$1.1x10^{14}$ 0.139	$6.3x10^{14}$ 0.797	$5.9x10^{14}$ 0.747
HCl			$1.3x10^{12}$ 0.0015	$<7.7x10^{11}$ 0.000895	$3.6x10^{13}$ 0.042	$8.1x10^{13}$ 0.094	$4.1x10^{12}$ 0.0048
CF_3COOH	$1.5x10^{13}$ 0.0375		$7.0x10^{12}$ 0.0175	$7.7x10^{12}$ 0.0193	$1.1x10^{13}$ 0.0275	$1.1x10^{12}$ 0.00275	$1.7x10^{12}$ 0.00425
NO_2	$< 3.3x10^{12}$ 0.00465	$1.7x10^{13}$ 0.0239	$< 4.5x10^{12}$ 0.0063	$1.3x10^{13}$ 0.0183	$5.3x10^{12}$ 0.00746	$2.2x10^{12}$ 0.00310	$5.6x10^{12}$ 0.00789
O_3	SS-reaction	$2.4x10^{14}$ 0.324	$4x10^{12}$ 0.00540	$3.0x10^{13}$ 0.0405	$1.7x10^{15}$ 2.30	$3.3x10^{14}$ 0.446	$3.2x10^{15}$ 4.324

However, the emphasis of the presentation will be placed on the reducing properties of the reference soot and MWCNT materials as indicated by the reactivity with O_3 and NO_2. These reducing surface functional groups may be part of a reversible redox-active catalytic system that uses air oxygen for oxidation of biochemical molecules in the presence of the carbonaceous nanomaterial of interest. Examples are the oxidative coupling of dithiothreitol (DTT) and the oxidation of dichlorodihydrofluorescein (DCFH) to dichlorofluorescein (DCF) which is fluorescing with amorphous carbon and soot. The reaction mechanism, reaction (a), (b) and (c) with (d) being the sum, is as follows:

$$O_2 + PM_{red} \rightarrow H_2O_2 + PM_{ox} \quad \text{(a)}$$
$$PM_{ox} + Red \rightarrow PM_{red} + Ox \quad \text{(b)}$$
$$\underline{H_2O_2 + PM \rightarrow PM_{oxx} + H_2O} \quad \text{(c)}$$
$$O_2 + Red + PM \rightarrow Ox + PM_{oxx} + H_2O \quad \text{(d)}$$

Reaction (d) indicates that Red corresponding to an oxidizable thus reducing biomolecule (such as an antioxidant) may be catalytically oxidized by O_2 to Ox in the presence of PM (amorphous carbon or soot) that is cycling between its reduced and oxidized form, PM_{red} and PM_{ox}, respectively. Reaction (c) describes the slow deactivation of the catalyst we have observed in laboratory studies. These results are interesting as they enable the possibility of predicting the condensed phase reactivity of aqueous aerosol suspensions with biologically relevant reducing agents on the basis of simple gas phase titration with NO_2 probing for strongly reducing sites. In a wider context harmful effects of nanoparticles on health have been mostly attributed to the **oxidative** properties of the aerosols. This work tries to draw attention to the fact that **reducing** properties of aerosols may be of even greater importance owing to a possible catalytic effect of nanoparticles in biochemical oxidations where the oxidant is air oxygen. The enclosed figure shows an example of such a catalytic oxidation of the prototypical antioxidant molecule Dithiothreitol ($C_4H_8O_2S_2$) to its cyclic (oxidized) form in the presence of molecular oxygen in aqueous solution and a suspension of FW2 amorphous carbon. Reaction (a) is the rate-limiting step controlling the overall kinetics.

In summary, we have searched for evidence of reducing surface functional groups on carbonaceous nanoparticles and have stumbled upon a catalytic reaction involving air oxygen that oxidizes biochemically relevant antioxidant molecules. Indeed, we have found evidence for the importance of reducing surface functional groups such as reaction (a) above that is rate-limiting and therefore shows up in correlation plots. However, these reducing groups do not act by themselves but in concert with oxidation reactions such as reaction (b) above. The concerted action of reactions (a) and (b) very efficiently catalytically oxidize biochemically active molecules such that a small number of catalytically active sites on the surface of carbonaceous nanoparticles max oxidize a large number of antioxidants, given the unlimited supply of the oxidizer air. Reaction (c) limits the turnover (number of catalytic cycles per site) owing to slow deactivation of the active catalytic site with time.

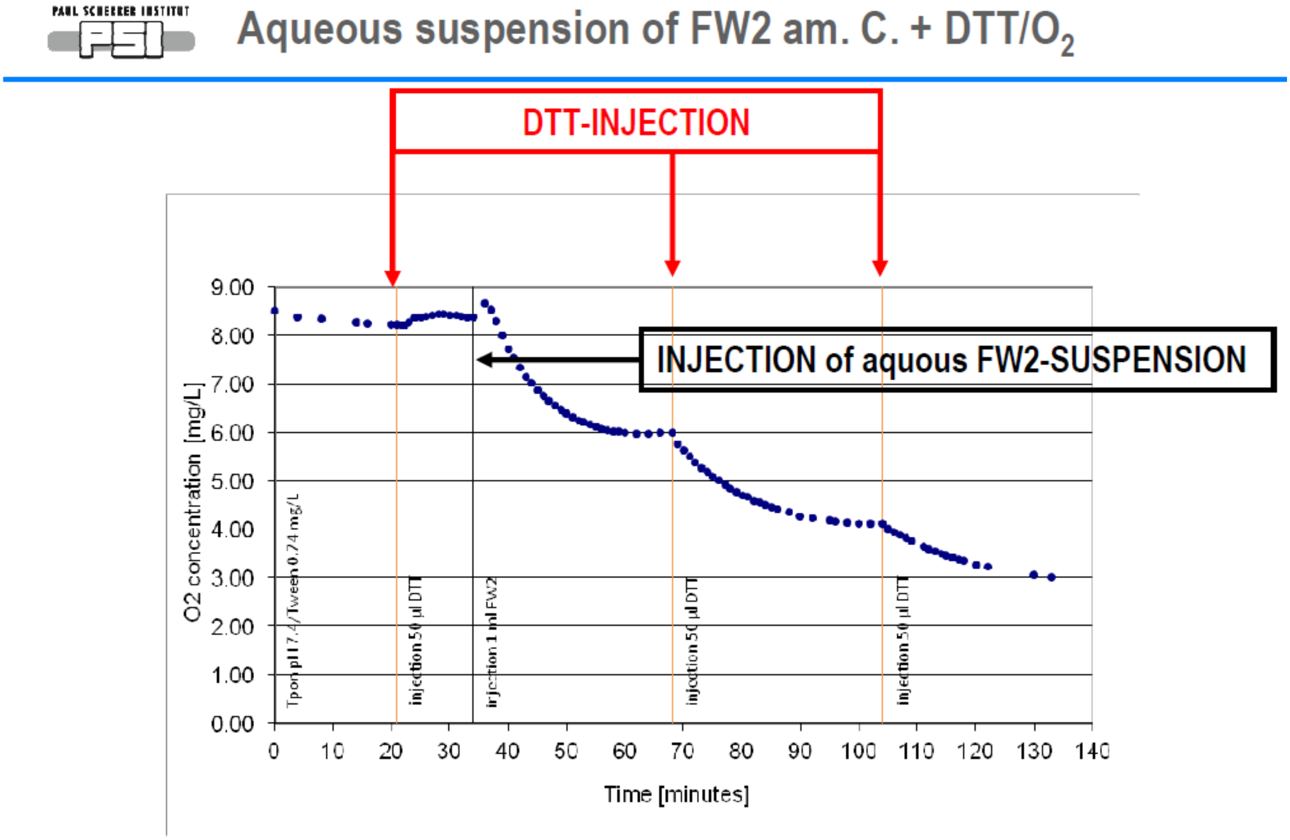

O_2 consumption measured using a Clark electrode upon repeated injection of DTT serving as a model compound to be oxidized by air oxygen dissolved in the aqueous solution in the presence of catalytic amounts of amorphous carbon FW2. The plot shows that oxidation of DTT starts only after the addition of the aqueous FW2 suspension.

We may summarize the present findings as follows:

- Surface Composition of Soot and other carbonaceous NP‘s is **multifunctional**.
- Use of „**chemical“ surface interrogation** techniques delivers different results in comparison with spectroscopic and imaging methods
- **Correlation** of surface composition in terms of number of surface functional groups with toxicological tests/biomarkers. An even **better correlation** may be obtained when considering the surface reactivity of probe gases instead of the number of active sites reacting with a probe gas.
- In addition to well-documented health effects of oxidized surface groups there are indications that **reduced** surface groups may lead to same. Incidence of NP-catalyzed chain reactions with NP as chain carrier/catalyst. Therefore, the oxidizing and reducing surface groups do not act in isolation, instead they are cycling between oxidized and reduced form an self-sustained efficient catalytic reaction system.

Wir schaffen Wissen – heute für morgen

Paul Scherrer Institut

Ari Setyan[1], Jean-Jacques Sauvain[2], Michael Riediker[2], Olga Popovicheva[3] and Michel J. Rossi[4]

[1]ULCO, Dunkerque(F); [2]IST Lausanne (CH); [3]Moscow State University; [4]PSI/LAC Villigen (CH)

Functional Groups on the Surface of Carbonaceous Nanomaterials and Human Health

PSI, 17. Juli 2013

Various Ways of Characterizing Soot Particles

- Thermal Behavior: Pyrolysis, oxidation, thermogravimetric measurement

- Extraction Behavior: Organic Phase vs. Elemental Carbon (OC/EC) or WSOC/WinSOC, etc.

- Elemental Analysis (C, H, N, O, S,…)

- Surface Spectroscopies (FTIR, XRD, EELS, XPS)

- Imaging (ESEM, HRTEM)

- **Chemical** Composition of the Interface: ➔ **Surface functional groups independent of chemical speciation.**

Gas Phase Probes for 4 Families of Surface Functions

$S\text{-}COOH + N(CH_3)_3$ ➔ $S\text{-}COO^-(CH_3)_3NH^+$ (Salt)

Oxidized surface

$S(R)\text{-}C{=}O + NH_2OH$ ➔ $S(R)\text{-}C(OH)(NHOH)$ ➔

$S(R)\text{-}C{=}N\text{-}OH$ (Imine, Schiff base) + H_2O

Partially oxidized surface (aldehydes, ketones)

$S\text{-}B{:} + HCl/CF_3COOH$ ➔ $S\text{-}B{:}H^+Cl^-/CF_3COO^-$ (Salt)

Basic oxides and (N-centered) bases

$S\text{-}C_{red} + O_3/NO_2$ ➔ $S\text{-}C_{ox} + O_2/N(II\text{ or }III)$ (HONO or NO)

Reduced adsorption sites, **strongly** reducing (NO_2) sites (subset), sum = strongly + weakly reducing sites (O_3)

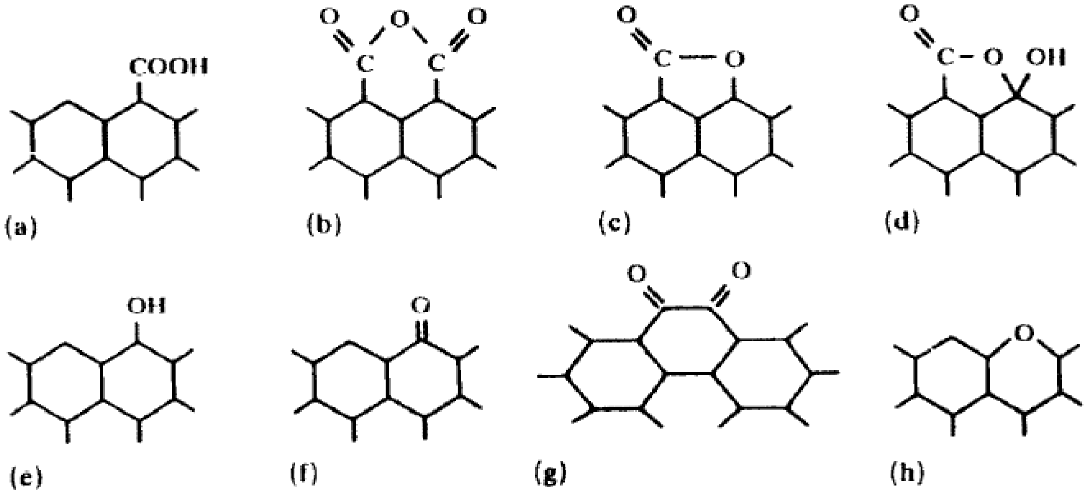

Fig. 1. Possible structures of surface oxygen groups (see text).

ACIDIC SITES

On carbonaceous particles

BASIC SITES

On carbonaceous particles (excluding N-bases!)

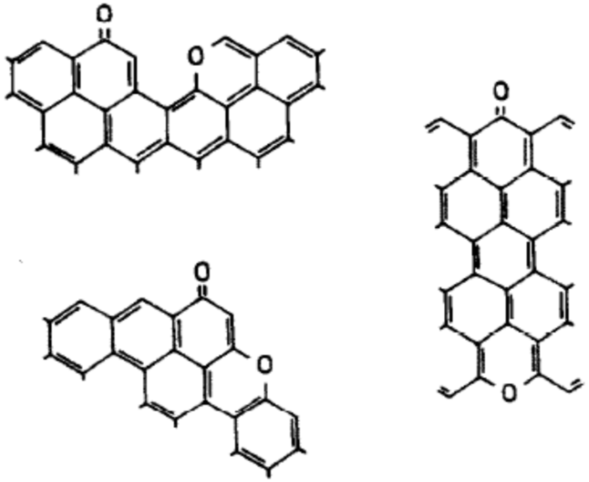

Fig. 5. Possible structures of basic surface sites on a graphene layer, derived from the γ-pyrone structure.

U. Hofmann et al; H.P. Boehm et al. (1970's)

Surface Interrogation using reactive probe Gases

Knudsen Flow reactor

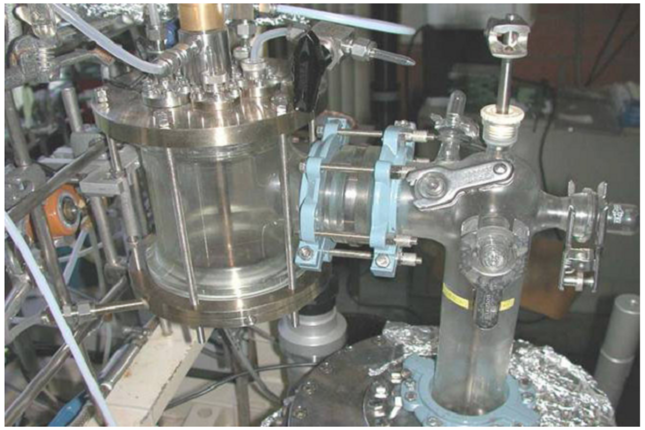

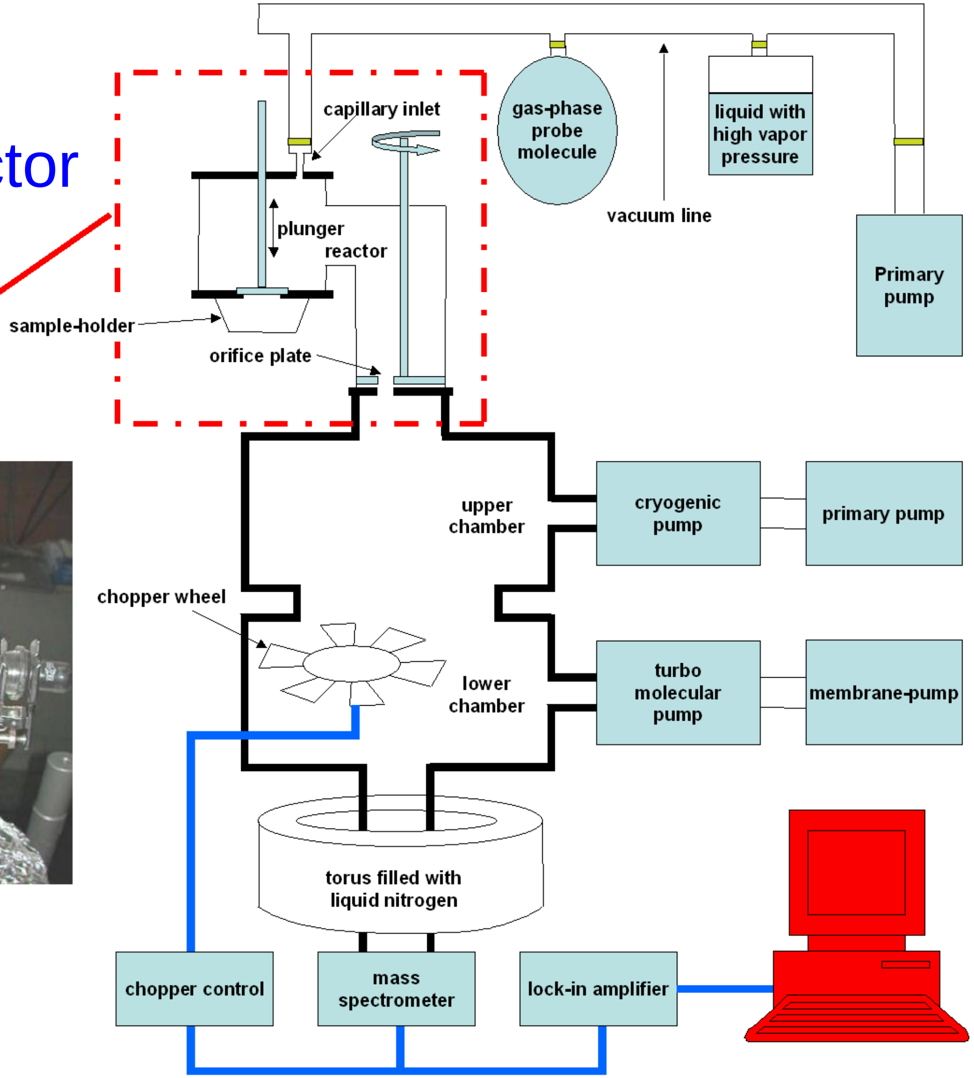

Two examples of raw data: Bus depot filter (top), hexane flame (bottom)

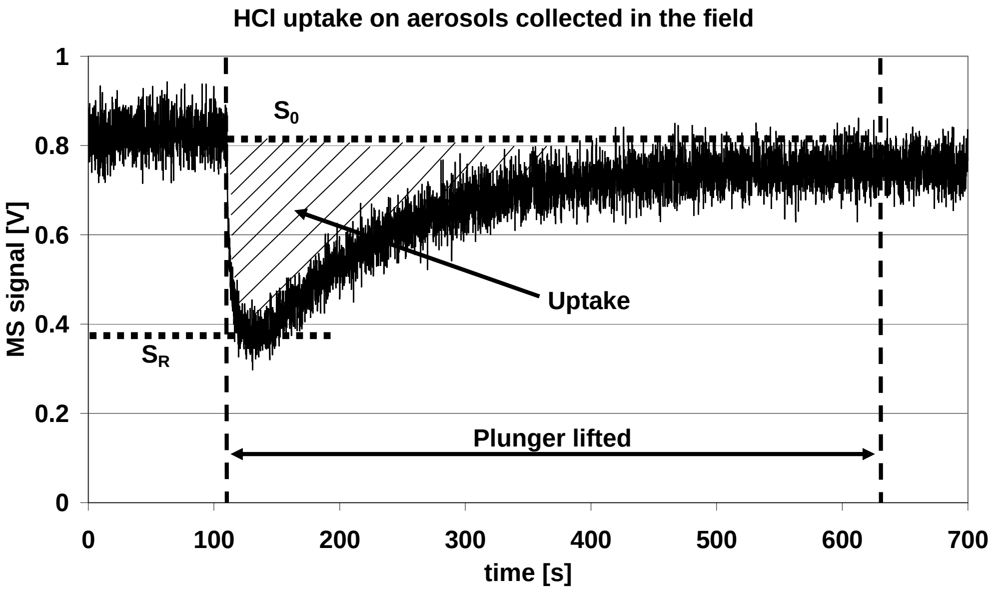

Typical raw data of a titration experiment using the Knudsen flow reactor. Sample: aerosols collected in the bus depot 2 (23.05.2006, daytime) on silanized quartz fiber filter. Probe gas: HCl. m/z: 36. S_0: mass spectrometer signal at steady state. SR: mass spectrometer signal immediately after the beginning of the reaction.

N_r(uptake) ➔ N_r/S (# cm^{-2})

N_r(uptake) ➔ N_r/M (# mg^{-1})

1ML coverage ➔ N_r/ML (# cm^{-2})

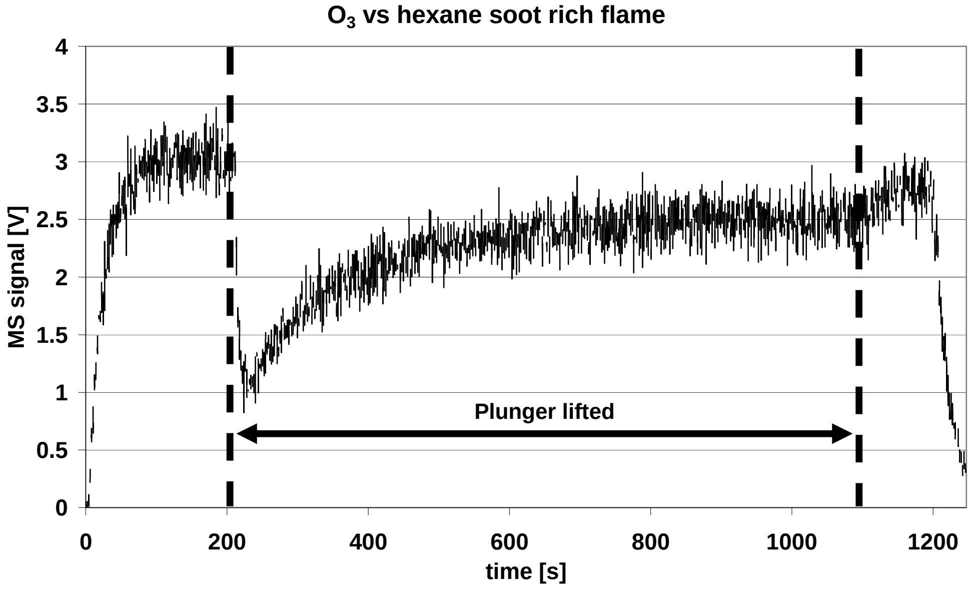

Raw data of O_3 uptake on 1.14 mg of soot from a rich hexane flame at a flow rate of 6.7×10^{15} molecule s^{-1} monitored at m/e 48 in the 1 mm diameter aperture Knudsen flow reactor ($k_{esc} = 0.0509$ s^{-1}) leading to the initial uptake coefficient $\gamma_0 = 1.6 \times 10^{-3}$.

UPTAKES of Probe Gases (N_i^M)

N_i^M/mg

N_i^M/cm^2

N_i^M/%ML

	Surface BET [m^2/g]	$N(CH_3)_3$	NH_2OH	CF_3COOH	HCl	O_3	NO_2
FS 101	20[a]	$5.8 \cdot 10^{14}$ $2.9 \cdot 10^{12}$ 0.81	$1.2 \cdot 10^{16}$ $6.0 \cdot 10^{13}$ 7.6	$1.8 \cdot 10^{15}$ $9.2 \cdot 10^{12}$ 2.3	No reaction	$7.3 \cdot 10^{17}$ $3.7 \cdot 10^{15}$ 498.0	$2.0 \cdot 10^{15}$ $9.8 \cdot 10^{12}$ 1.4
Printex 60	115[a]	$1.5 \cdot 10^{15}$ $1.3 \cdot 10^{12}$ 0.36	$2.1 \cdot 10^{16}$ $1.8 \cdot 10^{13}$ 2.3	$4.0 \cdot 10^{15}$ $3.5 \cdot 10^{12}$ 0.9	$8.2 \cdot 10^{14}$ $7.1 \cdot 10^{11}$ 0.08	$6.4 \cdot 10^{16}$ $5.6 \cdot 10^{13}$ 7.5	$7.4 \cdot 10^{15}$ $6.4 \cdot 10^{12}$ 0.90
FW 2	460[a]	$2.4 \cdot 10^{17}$ $5.2 \cdot 10^{13}$ 14.5	$4.4 \cdot 10^{17}$ $9.6 \cdot 10^{13}$ 12.2	$4.5 \cdot 10^{16}$ $9.9 \cdot 10^{12}$ 2.5	No reaction	$4.4 \cdot 10^{17}$ $9.6 \cdot 10^{13}$ 12.9	$4.1 \cdot 10^{16}$ $8.9 \cdot 10^{12}$ 1.3
SRM 2975	91	$4.9 \cdot 10^{16}$ $5.3 \cdot 10^{13}$ 14.7	$1.3 \cdot 10^{18}$ $1.5 \cdot 10^{15}$ 191.1	No reaction	$2.4 \cdot 10^{15}$ $2.6 \cdot 10^{12}$ 0.3	$8.3 \cdot 10^{15}$ $9.1 \cdot 10^{12}$ 1.2	$3.2 \cdot 10^{15}$ $3.5 \cdot 10^{12}$ 0.49
Diesel TPG	53.2	$3.1 \cdot 10^{16}$ $5.8 \cdot 10^{13}$ 16.1	$1.4 \cdot 10^{18}$ $2.6 \cdot 10^{15}$ 331.2	No reaction	$4.6 \cdot 10^{16}$ $8.7 \cdot 10^{13}$ 10.1	$1.3 \cdot 10^{17}$ $2.5 \cdot 10^{14}$ 33.7	$1.3 \cdot 10^{16}$ $2.4 \cdot 10^{13}$ 3.4
Hexane soot from rich flame	48.9	$1.8 \cdot 10^{15}$ $3.8\ 10^{12}$ 1.1	$2.1 \cdot 10^{17}$ $4.4\ 10^{14}$ 55.7	$1.8 \cdot 10^{15}$ $3.8\ 10^{12}$ 0.9	$9.0 \cdot 10^{15}$ $1.9\ 10^{13}$ 2.2	$9.5 \cdot 10^{17}$ $2.0\ 10^{15}$ 266.4	$2.6 \cdot 10^{16}$ $5.4\ 10^{13}$ 7.6
Hexane soot from lean flame	74.3	$2.8 \cdot 10^{15}$ $3.8\ 10^{12}$ 1.1	$3.3 \cdot 10^{17}$ $4.5\ 10^{14}$ 56.8	$3.2 \cdot 10^{15}$ $4.3\ 10^{12}$ 1.1	$3.1 \cdot 10^{15}$ $4.2\ 10^{12}$ 0.5	$2.0 \cdot 10^{18}$ $2.7\ 10^{15}$ 364.0	$1.9 \cdot 10^{16}$ $2.6\ 10^{13}$ 3.6

Surface Titration of Soot Reference / MWCNT Materials

Samples → Probes ↓	Graphitized Thermal Soot GTS6 (6 m^2/g)	Thermal Soot T900 (6.5 m^2/g)	Graphitized Thermal Soot GTS80 (80 m^2/g)	GTS80 + 5% BTA (80 m^2/g)	MWCNT 1 Uncoated (227.4 m^2/g))	MWCNT 2 Polyacid Polmer Coating (54.1 m^2/g)	MWCNT 3 PS-PB-PMMA Coating (34 m^2/g)
$N(CH_3)_3$			$1.1x10^{12}$ 0.0030	$6.1x10^{13}$ 0.1690	$1.3x10^{12}$ 0.0036	$1.2x10^{13}$ 0.033	$8.0x10^{11}$ 0.0022
NH_2OH			$4.0x10^{12}$ 0.005	$2.9x10^{13}$ 0.037	$1.1x10^{14}$ 0.139	$6.3x10^{14}$ 0.797	$5.9x10^{14}$ 0.747
HCl			$1.3x10^{12}$ 0.0015	$<7.7x10^{11}$ 0.000895	$3.6x10^{13}$ 0.042	$8.1x10^{13}$ 0.094	$4.1x10^{12}$ 0.0048
CF_3COOH	$1.5x10^{13}$ 0.0375		$7.0x10^{12}$ 0.0175	$7.7x10^{12}$ 0.0193	$1.1x10^{13}$ 0.0275	$1.1x10^{12}$ 0.00275	$1.7x10^{12}$ 0.00425
NO_2	$< 3.3x10^{12}$ 0.00465	$1.7x10^{13}$ 0.0239	$< 4.5x10^{12}$ 0.0063	$1.3x10^{13}$ 0.0183	$5.3x10^{12}$ 0.00746	$2.2x10^{12}$ 0.00310	$5.6x10^{12}$ 0.00789
O_3	SS-reaction	$2.4x10^{14}$ 0.324	$4x10^{12}$ 0.00540	$3.0x10^{13}$ 0.0405	$1.7x10^{15}$ 2.30	$3.3x10^{14}$ 0.446	$3.2x10^{15}$ 4.324

Hypothesis: Role of reduced surface sites

- Atmosphere is **oxidizing**: Trend to long-term oxidation of organics ➔ Atmospheric Aerosol surface believed to be oxidized ➔ Health Effects of Aerosols due to oxidized surface functional groups or molecules.
- Few reports on Correlation of health markers with **reducing capacity** of carbonaceous NP‘s:
  - Berg et al. in Chem. Res. Toxicol. 2010, *23*, 1874-1882.
  - Experimental results of Setyan, 2009 (PhD thesis, UNI Lausanne)

    ◊ Correlation of 8OHdg (urinary biomarker) with no. of reducing surface sites/cm^2 on carbonaceous NP‘s sampled in bus depot.

    ◊ Even better correlation with uptake kinetics (uptake coefficients) of probe gas with NP surface: O_3(+), $N(CH_3)_3$(-), NH_2OH(+), CF_3COOH(+), HCl(+).
- **Hypothesis: Reducing Capacity** of NP-interface may lead to negative health outcomes. **Reactivity (γ)** more important than abundance of sites.

Reactive Site density and uptake coefficient of amC for O_3

Correlation of no. of sites $N_i(O_3)$ reacting with O_3 (= reducing sites) vs.relative 8OHdg change in non-smokers

Correlation of uptake coefficient γ (= interfacial reactivity of probe gas) vs. relative 8OHdg change in non-smokers

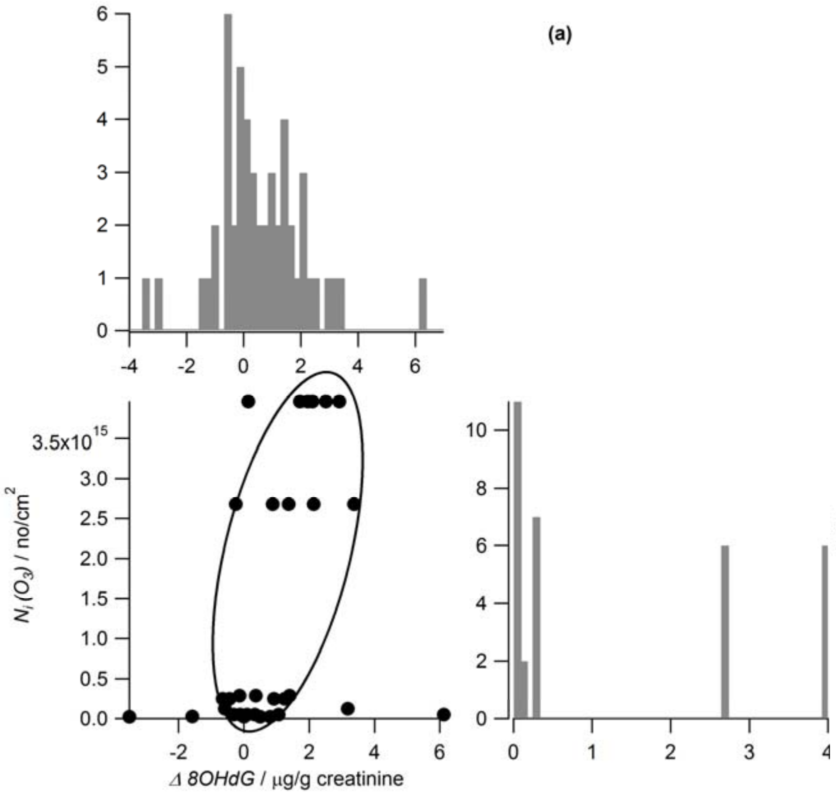

Number of sites

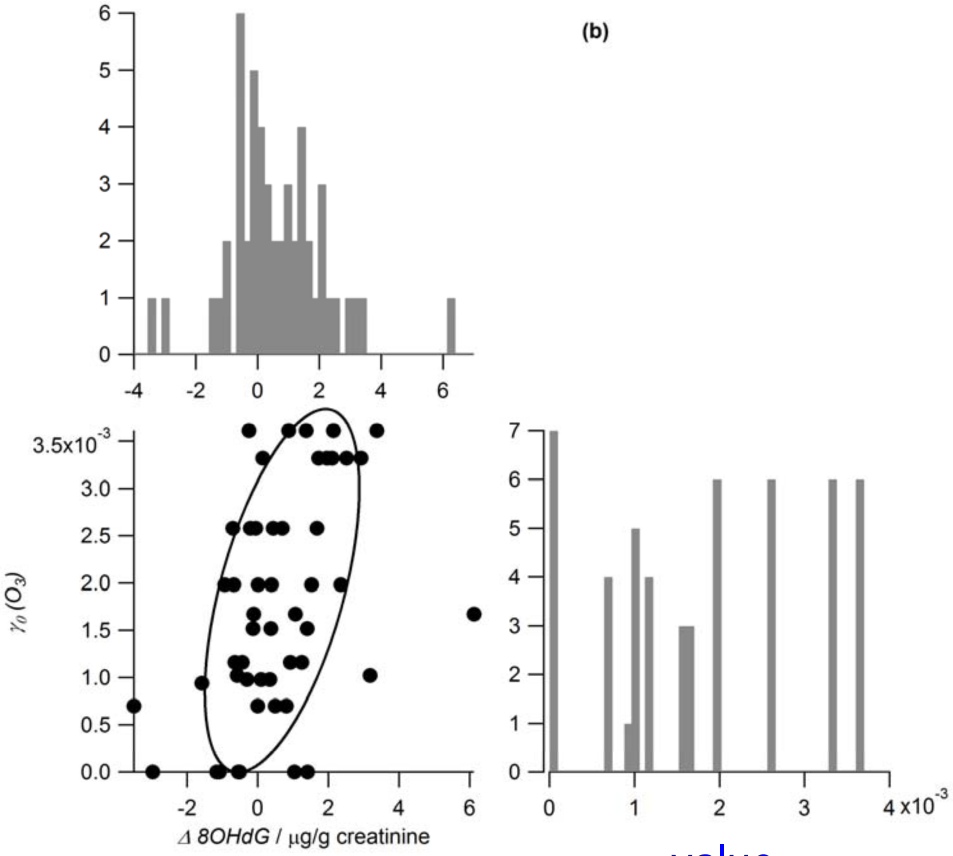

γ value

Three typical probe reactions for oxidized surface sites

Mild reducing agents = „Red“

2e-transfer systems

DTT (Dithiothreitol)

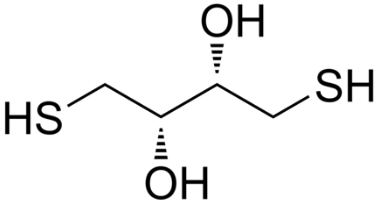

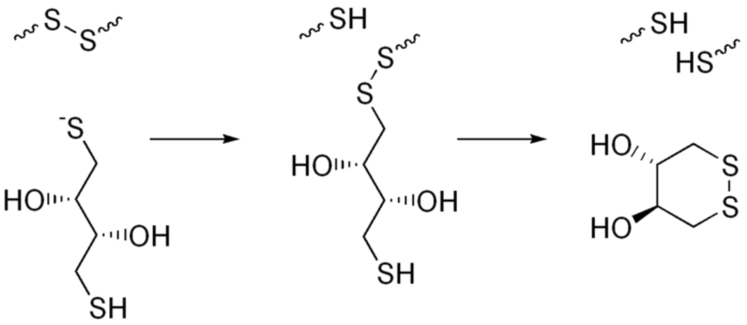

ONLY the monoanion of DTT is oxidized

L-Ascorbic Acid or Vitamin C

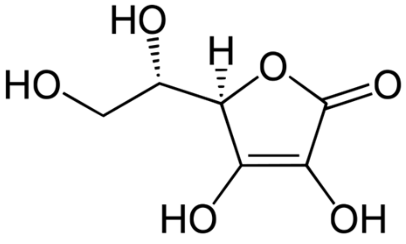

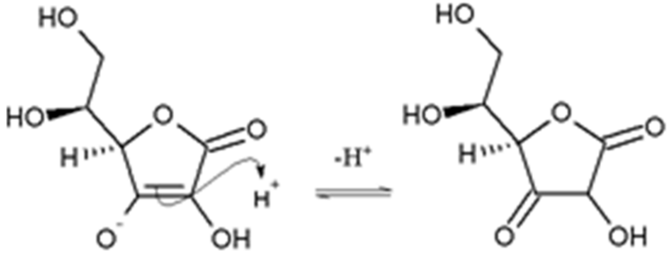

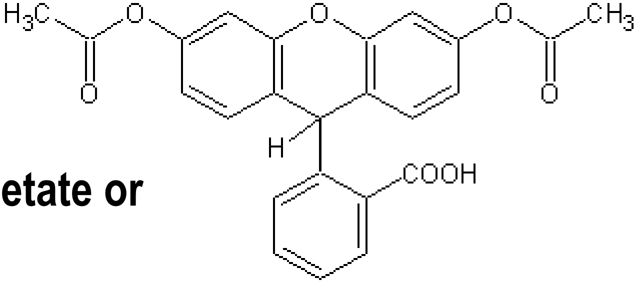

Dihydrofluorescein (diacetate or dichlorosubst.)

Oxidized form is FLUORESCENT

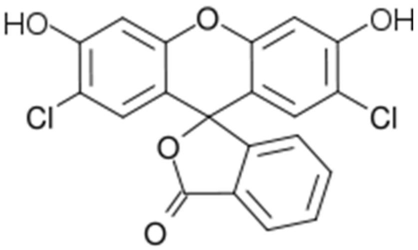

2,7-Dichlorofluorescein is oxidized form (lactol)

O_2 consumption kinetics in presence of „Red“, am. C NP‘s

0.100 mM DTT, 28 mg/L FW2 in suspension

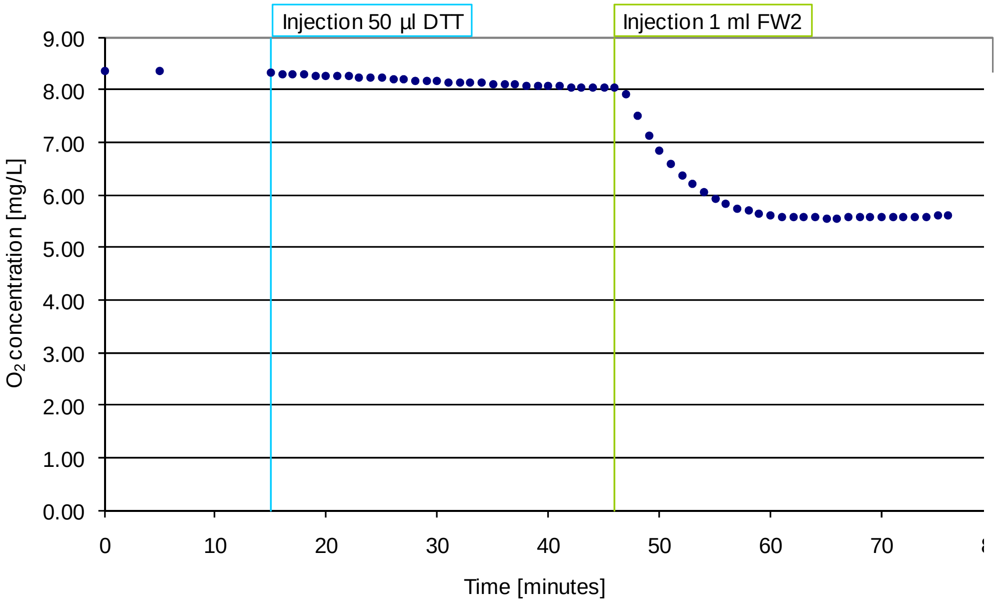

L-Ascorbic acid (Vitamin C),
FW2, Printex 60

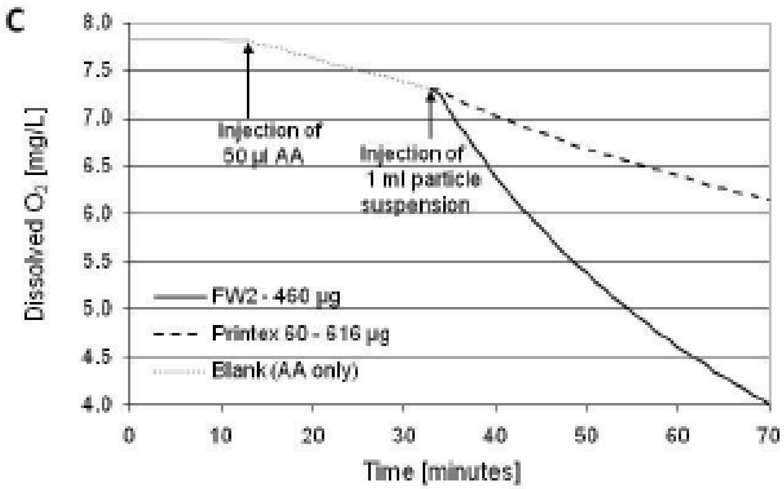

Relationship between O_2 consumption and strongly reducing (NO_2) and total reducing sites on FW2: ΔO_2 consumption is 2.5 mg/L or 4.7×10^{19} #/L for 1.2×10^{18} #/L strongly, 1.2×10^{19} total reducing sites. ΔO_2 is roughly equimolar with 6×10^{19} #DTT/L leading to bimolecular (experimentally confirmed) kinetics. There is a shortfall of strongly reducing (NO_2 probe) and total (O_3 probe) reducing sites on FW2 by a factor of 40 and 4, respectively.

The oxidation of DTT is therefore catalytic in FW2 soot nanoparticles.

Oxidation of DTT by O_2 w/o catalyst is slow: $DTT(Red)+O_2 \rightarrow Ox+H_2O_2$

Yield Ratios and Rate Law: RATE ^{DTT} = $k[O_2]$ [DTT] [CB]

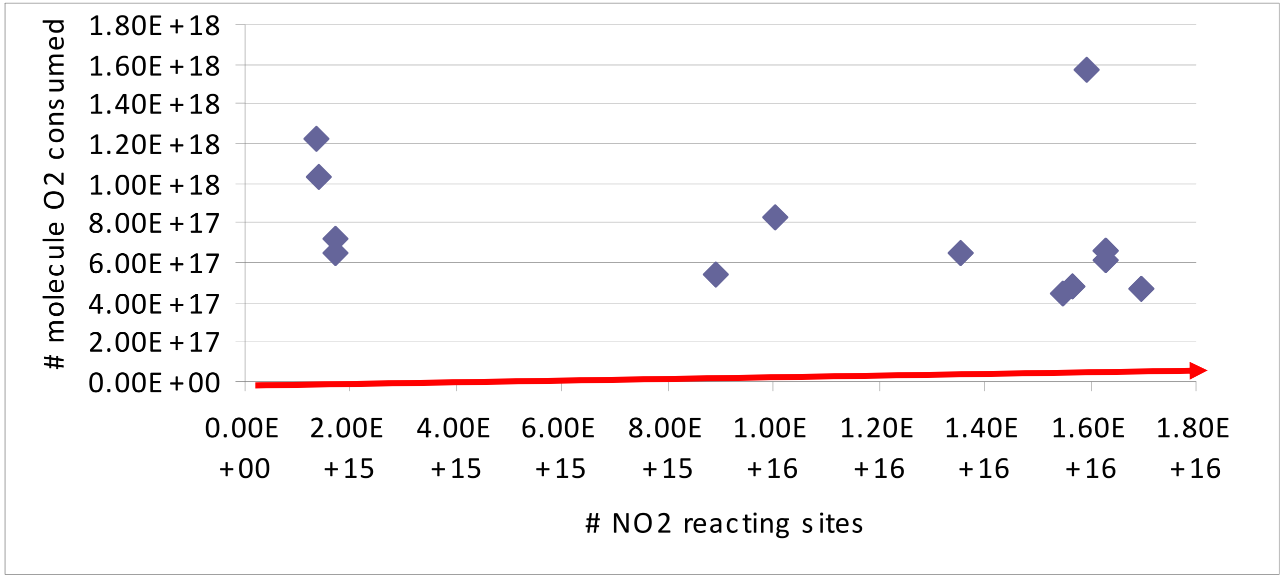

Stoichiometric line (1:1)

Between O_2 and DTT consumed in the presence of the amC catalyst

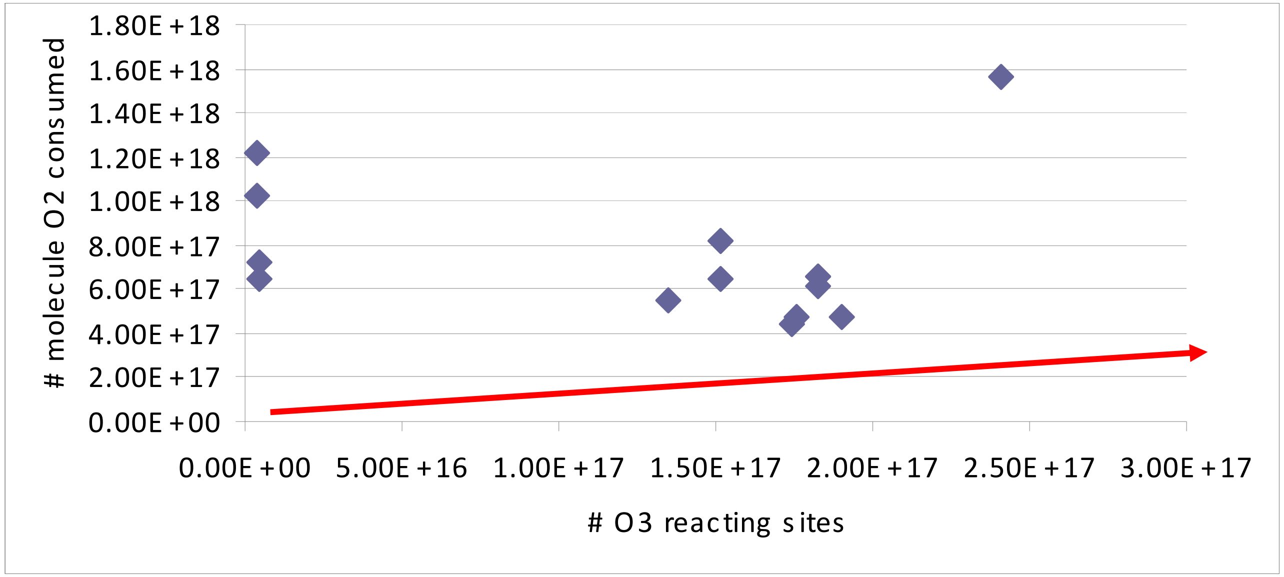

Every point above the red line represents „excess“ O_2 consumed in oxidation of „Red“ (reducing agent) in the presence of amC:

O_2 + 2Red ➔ 2Ox + $2H_2O$

Aqueous suspension of FW2 am. C. + DTT/O_2

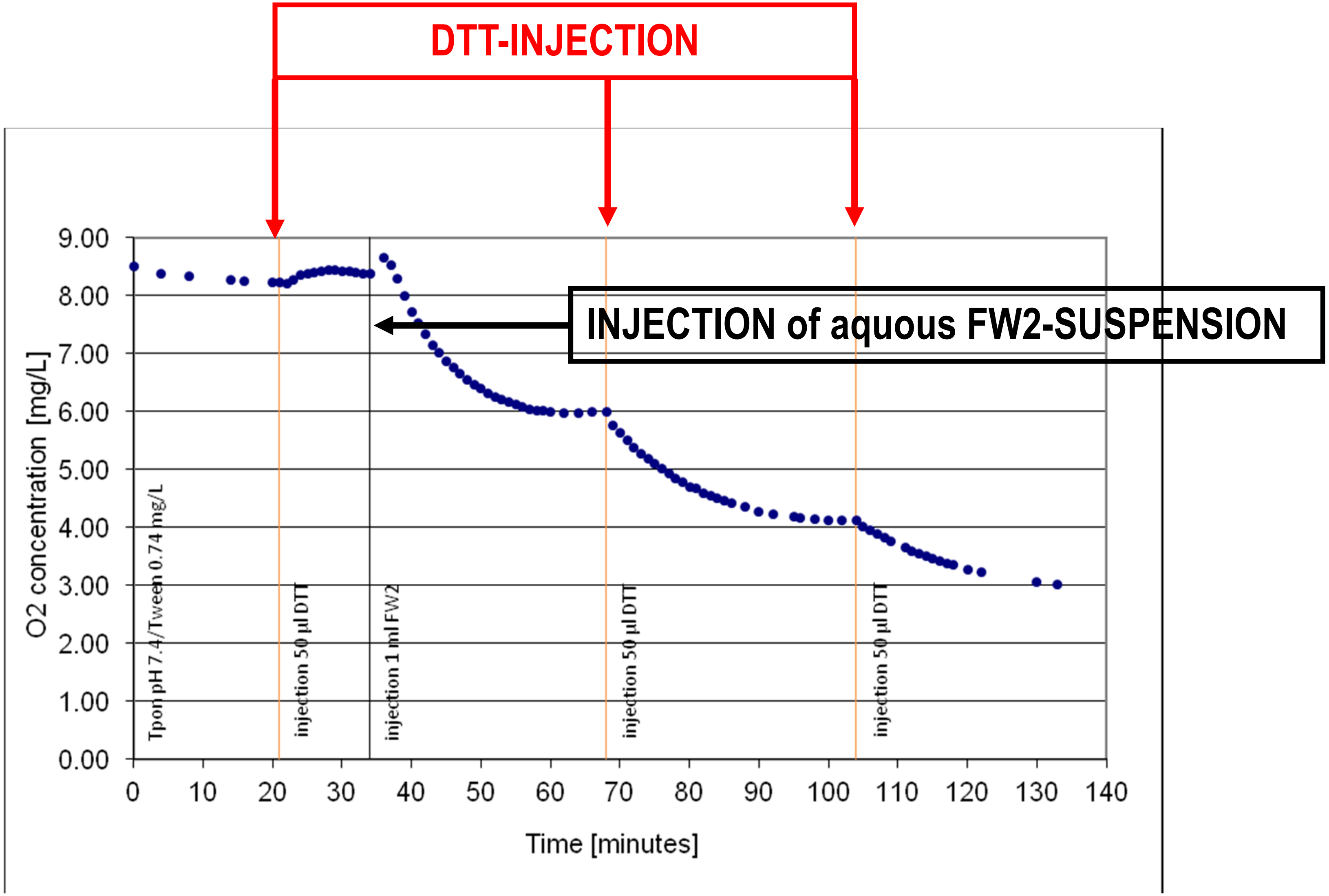

DTT-INJECTION

INJECTION of aquous FW2-SUSPENSION

Correlation: DCFH reactivity vs. # strongly **reducing** sites

Positive Correlation of DCFH reactivity with # of strongly reducing surface sites

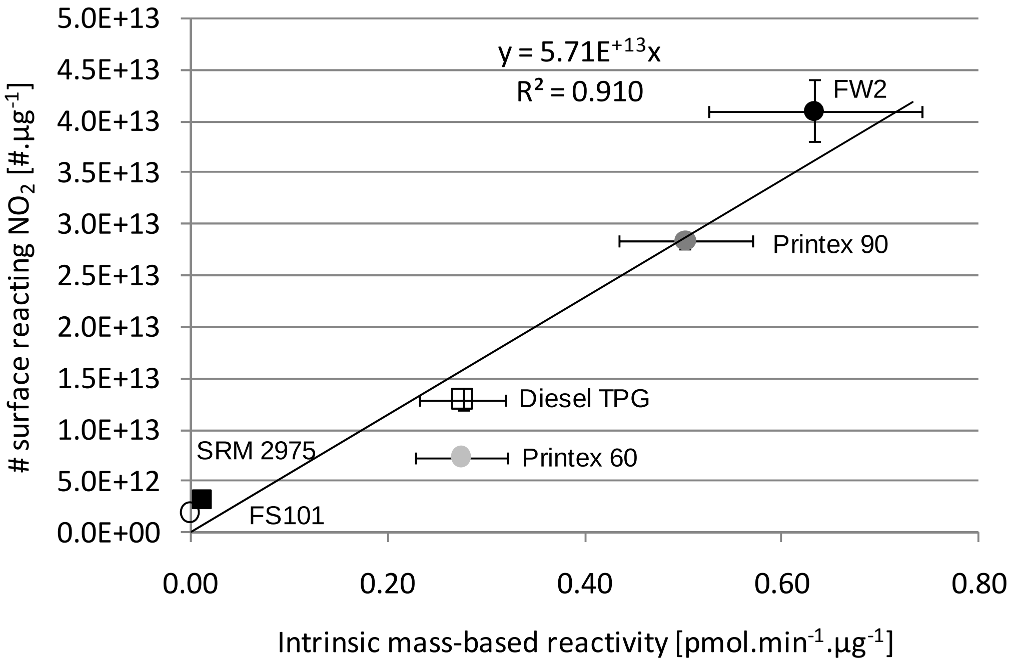

No correlation with oxidized and partially oxidized sites ($N(CH_3)_3$, NH_2OH-titration)

Correlation of DCFH reactivity with # of all reducing sites (O_3) is less good than with strongly-reducing sites (NO_2), $R^2 = 0.720$

NO_2 titration reveals strongly-reducing sites

This is not what we expected: DTT and/or DCFH reactivity is expected to correlate with # of oxidized or partially oxidized adsorption sites. How can we understand?

Look at quantitative aspects of kinetics, surface sites and stoichiometry.

Reaction Stoichiometry for oxidation of reducing agents

Detailed Mechanism satisfying the measured stoichiometry for O_2 consumption in acellular toxicity tests
(all reaction equations correspond to either two-hydrogen or two-electron transfer processes):

RATE LAW: DTT = k[O2] [DTT] [CB]

$\mathrm{PM_{red}} + \mathrm{O_2} \rightarrow \mathrm{PM_{ox}} + \mathrm{H_2O_2}$

$\mathrm{PM_{ox}} + \mathrm{Red} \rightarrow \mathrm{PM_{red}} + \mathrm{Ox}$

$\mathrm{aH_2O_2} + \mathrm{aRed} \rightarrow \mathrm{aOx} + \mathrm{2aH_2O}$

$\underline{\mathrm{(1\text{-}a)H_2O_2} + \mathrm{(1\text{-}a)PM} \rightarrow \mathrm{(1\text{-}a)PM_{oxx}} + \mathrm{2(1\text{-}a)H_2O}}$

$\mathrm{O_2} + \mathrm{(1+a)Red} + \mathrm{(1\text{-}a)PM} \rightarrow \mathrm{(1+a)Ox} + \mathrm{(1\text{-}a)PM_{oxx}} + \mathrm{2H_2O}$

Rate-limiting step derived from correlation r vs. # sites

Competition of „Red“ vs. PM for H_2O_2

With a = 1 (simple mechanism) the stoichiometry becomes:

$\mathrm{O_2} + \mathrm{2Red} \rightarrow \mathrm{2Ox} + \mathrm{2H_2O}$

0.0 ≥ a ≥ 1.0

Branching Ratio

CONCLUSIONS – 4 Take-Home Lessons

- Surface Composition of Soot and other carbonaceous NP‘s is MULTIFUNCTIONAL
- Use of „chemical“ surface interrogation techniques delivers different results re spectrometric methods
- Correlation of surface composition in terms of surface functional groups with toxicological tests/biomarkers
- In addition to well-documented health effects of oxidized surface groups there are indications that REDUCED surface groups may do the same. Incidence of NP-based chain reactions with NP as chain carrier/catalyst

CONCLUSIONS

•Surface composition of the NP surface remains unaffected, instead air O_2 is effectively used to oxidize « Red ».

• Rate of « Red » oxidation correlates best with no. of surface sites reacting with NO_2, that is with strongly reducing sites.

• However, we set out to probe the oxidative capacity of the NP surface and therefore expected to titrate the PM_{ox} sites on the NP surface.

• The rate-limiting step in the catalytic reaction of « Red » oxidation by air O_2 in the presence of carbonaceous NP's is the oxidation of reduced surface groups (= oxidation of PM_{red} by O_2).

• Chain length of catalytic oxidation ranges from a few tens to a few hundreds depending on « Red ». Together with the branching ratio « a » these two parameters define the catalytic oxidation of « Red ».

Aerosol Surface Characterization

Three **Constraints** for observing a titration reaction:

- Reactions must be fast (time scale of $1/k_{esc}$ ~ 10 s)
- Reactions are occurring at low pressure: ~ 10^{-3} mbar
- Reactions must occur at ambient temperature

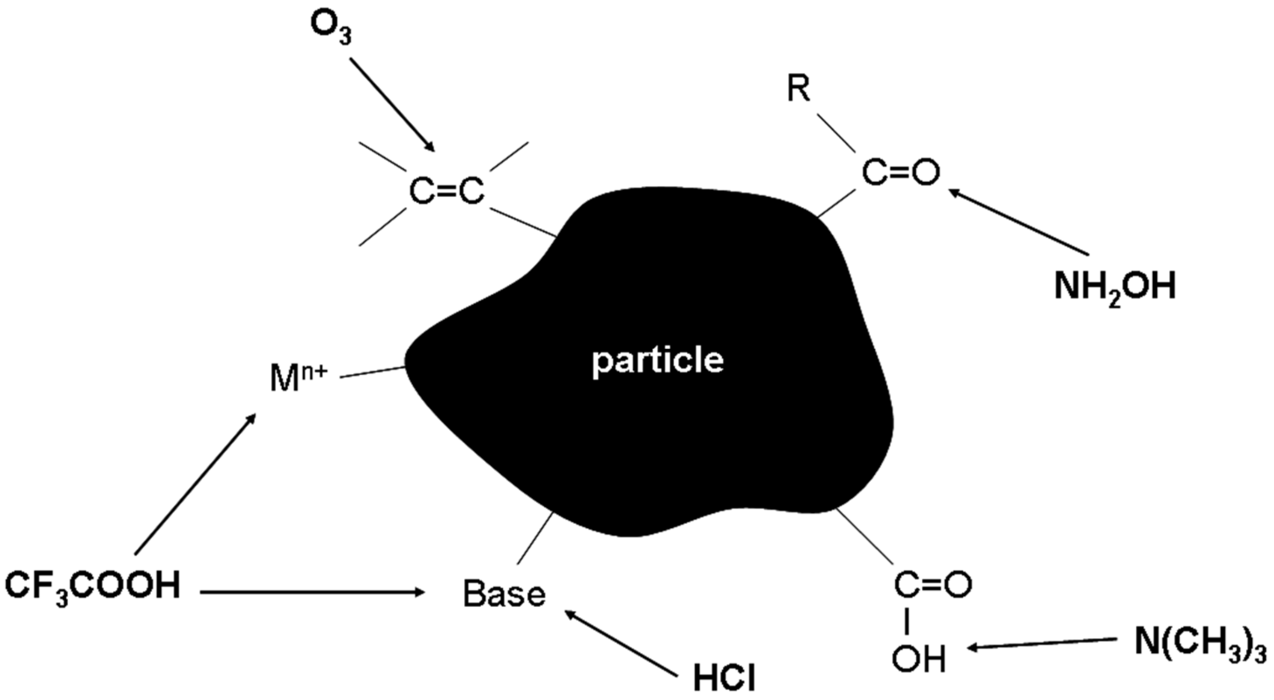

Comparison of GTS#3 and GTS#4

- Factor x50 more acidic (carboxylic) groups on soot #4 compared to soot #3 (TMA probe). Compare polyacrylic acid-coated MWCNT's (Tabet et al., P&FT 2011)which has x6 times less acidic sites compared to soot #4.
- Surprising abundance of partially oxidized sites (NH_2OH probe, aldehyde, ketone) increasing by x7.5 in going from soot #3 to soot #4. Are some of the deposited aromatic tricarboxylic acid molecules reduced to ketones/aldehydes by the reducing PM interface?
- Abundance of basic sites for both soot types. Propensity for TFA over HCl adsorption. This would indicate α- or γ-Pyrone-type (basic) oxides.
- Abundance of reducing sites of soot #4. Apparent coexistence between acidic and therefore highly oxidized (TMA probe) together with reducing (NO_2, O_3 probe) sites on the same interface.
- Sensitivity of the method is 2.5×10^{14} molecule mg^{-1} or 3×10^{11} molec cm^{-2} or 4×10^{-4} of a molecular monolayer for soot #4 (GTS80 with BET = 80 m^2/g).
- Both O_3 and NO_2 show steady-state uptake coefficients on the order of 3×10^{-5} for soot #3 and #4.
- Correlation between strongly-reducing (NO_2 probe) and all reducing (O_3 probe) sites.

Clark Electrode for the measurement of the O_2 consumption rate

Clark electrode

Closed arm with a silicone septum, allowing injection of solutions.

Closed arm with a silicone septum and a teflon lid.
Used as overflow during the injection of the solutions.

Magnetic bar

Magnetic plate

Volume: 14.1 ml

A: Pt-Electrode
B: Ag/AgCl Electrode
C: Sat. KCl Electrolyte
D: Thin Teflon Membrane
E: Rubber O-Ring
F: Voltage Supply
G: Galvanometer

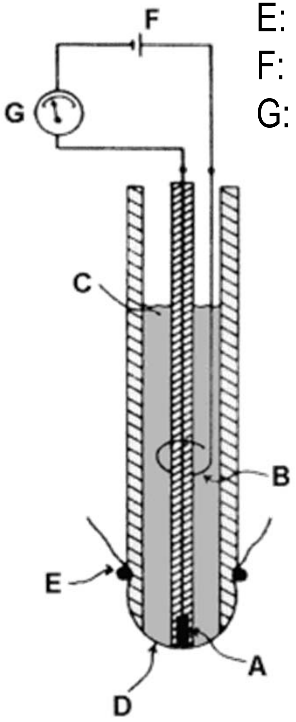

Cathode (reduction of O_2 at „A“):

$O_2 + 2H_2O + 4e^- \rightarrow 4OH^-$

Anode (oxidation of Ag^0 at „B“):

$\underline{4Ag + 4Cl^- \rightarrow 4AgCl + 4e^-}$

$4Ag+O_2+4Cl^-+2H_2O \rightarrow 4AgCl+4OH^-$

CONCLUSIONS

- Catalytic activity of carbonaceous NP's: dissolved O_2 oxidizes reducing agent „Red" instead of NP surface
- „Red" oxidation correlates with strongly reducing (PM_{red}), not oxidizing (PM_{ox}) NP surface sites
- NP is redox cycled (quinone-hydroquinone pair, no metal): Chain lengths of 40-800 O_2 per reducing site PM_{red}
- NP loss due to competition between irreversible oxidation of PM and oxidation of „Red" for H_2O_2. This leads to stoichiometry $[\Delta DTT]/[\Delta O_2] \leq 2.0$ ranging from 1.2 to 1.6 depending on type of amorphous carbon

Conventional Wisdom

PM leads to oxidative stress via production of ROS

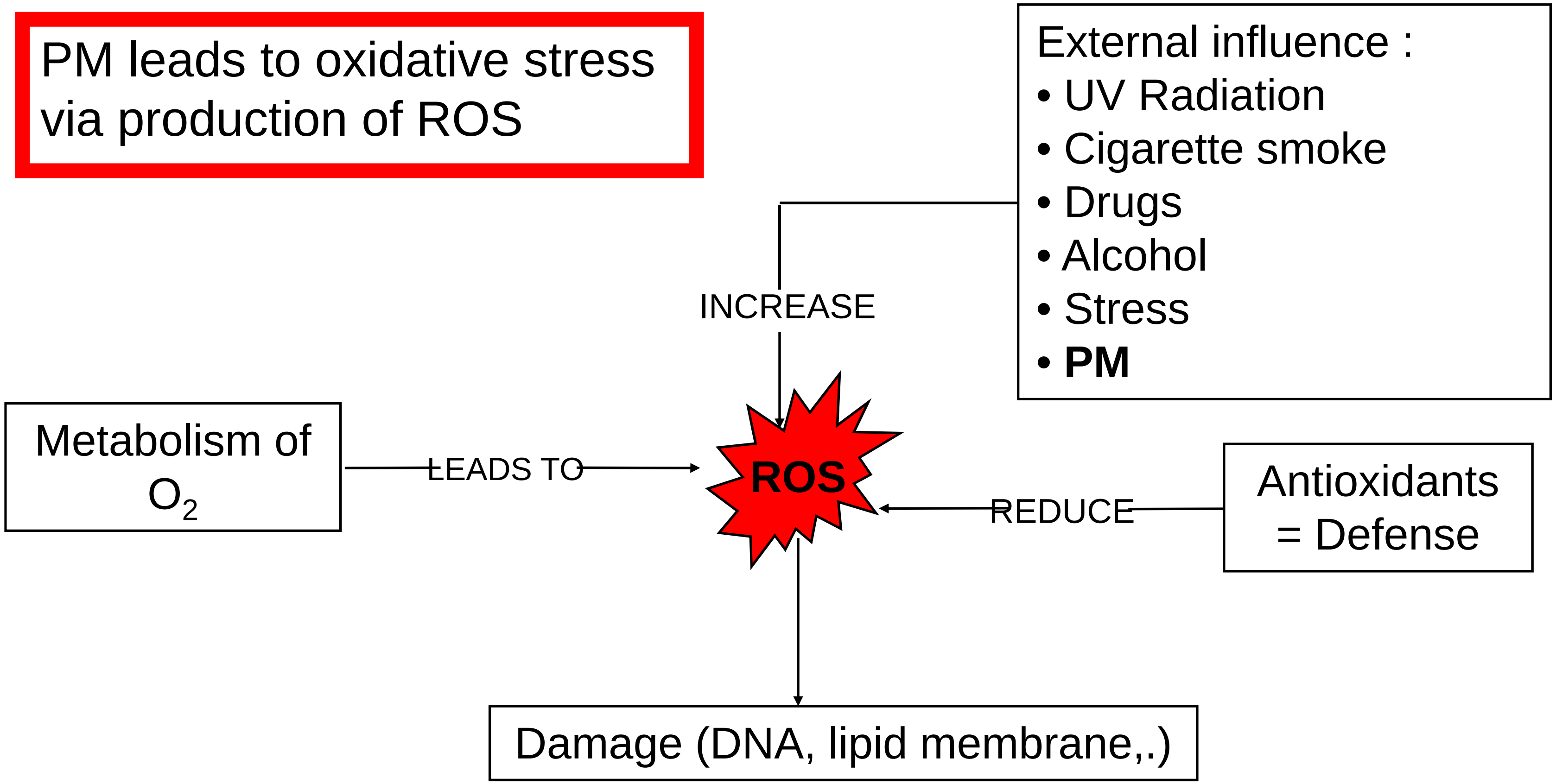

External influence :
- UV Radiation
- Cigarette smoke
- Drugs
- Alcohol
- Stress
- **PM**

ROS = Reactive Oxygen Species ($OH^\bullet$, $O_2^{\bullet-}$, singlet oxygen; H_2O_2, HO_2,…..)